



A field investigation of wind erosion in the farming–pastoral ecotone of northern China using a portable wind tunnel: a case study in Yanchi County

NAN Ling^{1,2*}, DONG Zhibao¹, XIAO Weiqiang¹, LI Chao¹, XIAO Nan¹, SONG Shaopeng¹, XIAO Fengjun¹, DU Lingtong³

¹ School of Geography and Tourism, Shaanxi Normal University, Xi'an 710119, China;

² Research Center for Western Development, Ningxia University, Yinchuan 750021, China;

³ Breeding Base for State Key Laboratory of Land Degradation and Ecological Restoration in Northwest China, Ningxia University, Yinchuan 750021, China

Abstract: The farming–pastoral ecotone in northern China is an extremely fragile ecological zone where wind erosion of cropland and rangeland is easy to occur. In this study, using a portable wind tunnel as a wind simulator, we conducted field simulated wind erosion experiments combined with laboratory analysis to investigate wind erosion of soils in trampled rangeland, non-tilled cropland and tilled cropland in Yanchi County, China. The results showed that compared with rangeland, the cropland had a higher soil water holding capacity and lower soil bulk density. The wind erosion rate of trampled rangeland was much higher than those of non-tilled cropland and tilled cropland. For cropland, the wind erosion rate of the soil after tilling was surprisingly less than that of the soil before tilling. With increasing of wind speed, the volume mean diameter of the eroded sediment collected by the trough in the wind tunnel generally increased while the clay and silt content decreased for all soils. The temporal variation in wind erosion of the trampled rangeland indicated that particle entrainment and dust emission decreased exponentially with erosion time through the successive wind erosion events due to the exhaustion of erodible particles.

Keywords: wind erosion rate; wind tunnel; eroded sediment; soil particle size; cropland; rangeland; semi-arid region

Citation: NAN Ling, DONG Zhibao, XIAO Weiqiang, LI Chao, XIAO Nan, SONG Shaopeng, XIAO Fengjun, DU Lingtong. 2018. A field investigation of wind erosion in the farming–pastoral ecotone of northern China using a portable wind tunnel: a case study in Yanchi County. *Journal of Arid Land*, 10(1): 27–38. <https://doi.org/10.1007/s40333-017-0073-8>

1 Introduction

Wind erosion is widespread over the land surface of Earth. It reduces agricultural sustainability in arid and semi-arid regions (Yang and Lu, 2016). Wind erosion has significant offsite effects and can greatly affect local and regional air quality by entraining fine particles (<100 µm in the case of an aerosol) and nutrients from the soil surface into the air (Zobeck and Van Pelt, 2011). In China, the total area of sandy desertification, caused primarily by wind erosion of soil, was 1.826×10^6 km² (Wang et al., 2008). This area accounted for >69.93% of the total desertification area in 2014, which also included waterpower desertification, saline desertification, and freeze–thaw desertification (State Forestry Administration, PR China, 2015).

*Corresponding author: NAN Ling (E-mail: nanling83@126.com)

Received 2017-06-08; revised 2017-10-12; accepted 2017-10-24

© Xinjiang Institute of Ecology and Geography, Chinese Academy of Sciences, Science Press and Springer-Verlag GmbH Germany, part of Springer Nature 2018

The farming–pastoral ecotone in northern China is the transitional zone between humid areas of traditional intensive cultivation and arid and semi-arid areas of rangeland (Zhou and Zhang, 1992). It is an extremely fragile ecological zone. Because of insufficient precipitation, the frequent occurrence of drought and strong winds in spring, as well as over-grazing and extensive reclamation of rangeland, the related aeolian processes are severe in the farming–pastoral ecotone in northern China (Zhu and Chen, 1994) and have been identified as the primary cause of soil degradation in this area (Yan et al., 2010). Some studies suggested that the cropland in the farming–pastoral ecotone is one of the major sources of dust (Dong et al., 2000; Liu et al., 2007), since tillage can break clods, weaken soil mechanical stability, and increase soil erodibility (Chepil, 1953; Chepil and Woodruff, 1954; Fryrear, 1981; Zobeck and Popham, 1990). Wind erosion of soil removes the fine soil particles (consisting mainly of clay, silt and organic matter), which are some of the most important soil constituents. Since both soil particle size and the proportions of sand, silt and clay are of primary importance to soil structure and stability (Chepil and Woodruff, 1954; Zhao et al., 2005), the preferential removal of fine particles is detrimental to the soil structure (Li et al., 2015). These fine particles also greatly influence the soil water holding capacity, so their removal could reduce soil moisture storage. Nutrient elements also tend to be attached to the fine particles, thus the loss of fine particles could reduce soil fertility (Zobeck and Popham, 1990; Sharratt et al., 2015). Overall, the loss of topsoil with fine particles due to wind erosion has a measurable effect on crop yields (Tang et al., 2016).

Wind erosion may be triggered and promoted by soil disturbance due to various activities such as cultivation, grazing and traffic (Liu et al., 2003; Li et al., 2004; Wang et al., 2011). The disturbance of soil crusts, for example by livestock trampling or tillage, can increase the amount of the eroded sediment (Baddock et al., 2011), and may also influence the entrainment threshold by changing the grain size distribution of soil on the surface (Belnap et al., 2007). Wind erosion can reduce soil productivity in a variety of ways. Specifically, fine soil particles containing nutrients are lost, and the remaining particles give the soil a coarser texture. The abrasion of shoots by soil particles during saltation can result in heavy damage to crops, which can be particularly serious in spring when crops sprout. The cultivation of cropland can greatly increase soil loss through wind erosion when compared to uncultivated cropland (Liu et al., 2007; Sharratt et al., 2010; Singh et al., 2012). Cultivation increases the erodible fraction and reduces the dry aggregate stability of medium-textured soils since these soils lack cementing agents (Colazo and Buschiazzi, 2010). For cropland, wind erosion of soil varies considerably after the tillage because a physical crust is formed by dew, which protects the soils from wind erosion (Segovia et al., 2017). For rangeland, animals trampling the soil also increases the mass of erodible fine particles (Baddock et al., 2011). An important approach reducing wind erosion of cropland is leaving crop residue in the field (Van Pelt et al., 2013). Conversion to conservation tillage with stubble management from conventional tillage significantly increases soil organic carbon in a relatively short period (Gao et al., 2016). The sediment transport amount during the growing season of crops in cultivated cropland of arid and semi-arid regions was low because of crop residue (Zhang et al., 2013).

Although wind erosion of cropland and rangeland is well understood, the erodibility of both land types in the same locality is still to be investigated. The goal of this study is to evaluate the wind erosion of cropland and rangeland in the farming–pastoral ecotone in northern China. To quantify soil stability and wind erosion rate, we integrated soil analyses with field simulated wind erosion experiments using a portable wind tunnel. The short-term dynamics of wind erosion were also analyzed.

2 Materials and methods

2.1 Study area

Field experiments were conducted at the Desert Steppe Ecosystem Experimental Research Base of Ningxia University (37°49'30"N, 107°29'22"E; 1410 m a.s.l.), which is located in Yanchi

County, Ningxia Hui Autonomous Region, China (Fig. 1a). The study area is characterized by a continental monsoon climate with mean annual precipitation of 250 mm, mean annual evaporation of 2180 mm, and annual mean temperature of 7.6°C. Average annual wind speed is 2.8 m/s, and the prevailing wind direction is from the northwest to the southeast. The mean occurrence of gale-force events (wind speed >17 m/s) is 30 d/a and the occurrence of sand storms and blowing dust events is 20 d/a (Zhang et al., 2013). The zonal soil is aeolian sandy soil derived from aeolian sediment. The vegetation types are shrub vegetation, meadow, steppe, and sandy or desert vegetation. Shrubs are dominated by *Salix psammophila* and *Caragana microphylla*, which have a high coverage and are widely distributed. The desert steppe is dominated by *Caragana tibetica*, *Oxytropis aciphylla*, *Nitraria sibirica* and *Kalidium foliatum* (Liu et al., 2015). The arid rangeland is dominated by *Stipa grandis*, *Stipa bungeana*, *Agropyron cristatum* and *Thymus serpyllum* var. *mongolicus*. In the study area, there are discontinuous areas of irrigated cropland around peasant houses and extensive rangeland lies beyond the cropland (Fig. 1b). Since 2003, the cropland has been cultivated with maize as the main crop in most years. Since 2011, the grazing intensity in the rangeland has been at the present level of about 2.5 sheep/hm².

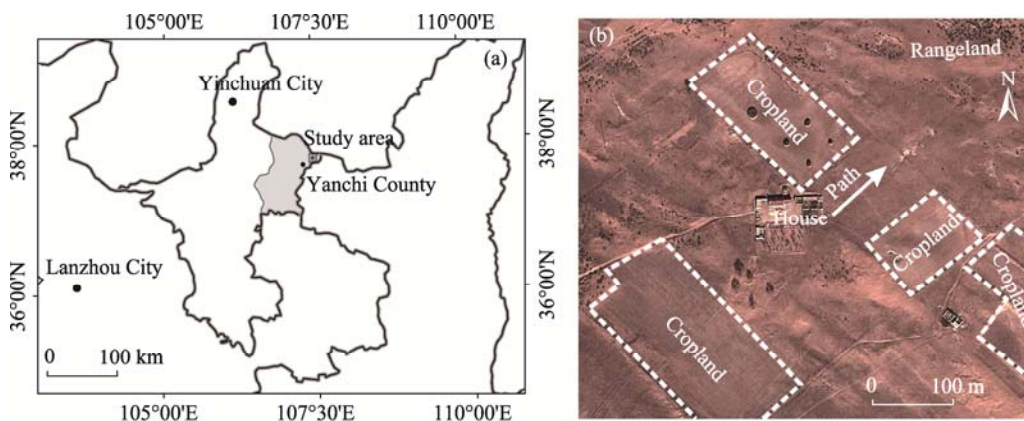


Fig. 1 Location of the study area (a) and spatial distributions of cropland and rangeland (b). Cropland is shown in the square with white dotted lines and rangeland lies beyond the cropland. It should be noted that rangeland mainly distributes at the northeast of the house and exceeds the scope of the figure.

2.2 Experimental design and *in-situ* experimental facility

In this study, a portable wind tunnel was used to investigate wind erosion of cropland and rangeland. The cropland treatments included non-tilled cropland (NTC) and tilled cropland (TC). The NTC was not ploughed after being harvested the previous year. The TC was loosened with a spade immediately before the field simulated wind erosion experiments were carried out. For rangeland, a severe trampled rangeland (TR) site on a path near the sheepfold was selected because it was normally trampled by sheep every day without any further artificial operation.

Field simulated wind erosion experiments were conducted in early April 2017 using a portable wind tunnel (Fig. 2). The portable wind tunnel enables quasi-natural wind erosion simulation under controlled conditions (Leys and Raupach, 1991) and provides dynamic and quantitative information on particle transport by wind erosion. The wind tunnel had a rectangular cross-section (0.4 m width×0.5 m height), with an open-floored working section up to 5.0 m long. The air flow in the tunnel was produced by a mixed flow blower controlled by a frequency changer. The mixed flow blower was connected to the leading end of the flow-straightening section by a flexible connection made of canvas. The wind speed could be varied from 0 to 22 m/s. At the end of the wind tunnel, a sediment collection trough (3 m wide, 5 m long and 1 m deep) constructed with polyvinyl chloride sheeting was used to make the eroded sediment deposited. Then, the eroded sediment was collected by a vacuum cleaner to obtain the weight and to test the dry particle size distribution (Fister and Ries, 2009). A DustTrak Aerosol Monitor 8533 (TSI Ltd., USA) was used to monitor the dust concentration (PM₁₀, mg/m³) during the experiments. The

inlet tube for the monitor was set at the end of the wind tunnel at a height of 10 cm. Data were collected at a frequency of 1 Hz. The wind speeds set for the experiments were 8, 12 and 16 m/s. Wind speed was measured at a height of 25 cm aboveground by a rotating vane anemometer. For TC and NTC, the blowing time was set as 10 min at each wind speed. For TR, the blowing time was also set as 10 min totally at each wind speed, but it was further divided into five 2-min intervals. After ending of every 10-min blowing event for TC and NTC and 2-min blowing event for TR, the eroded sediment in the trough was collected to weigh and test dry particle size distribution. There were five sets of data for TR and they were used to characterize the dynamics of wind erosion.

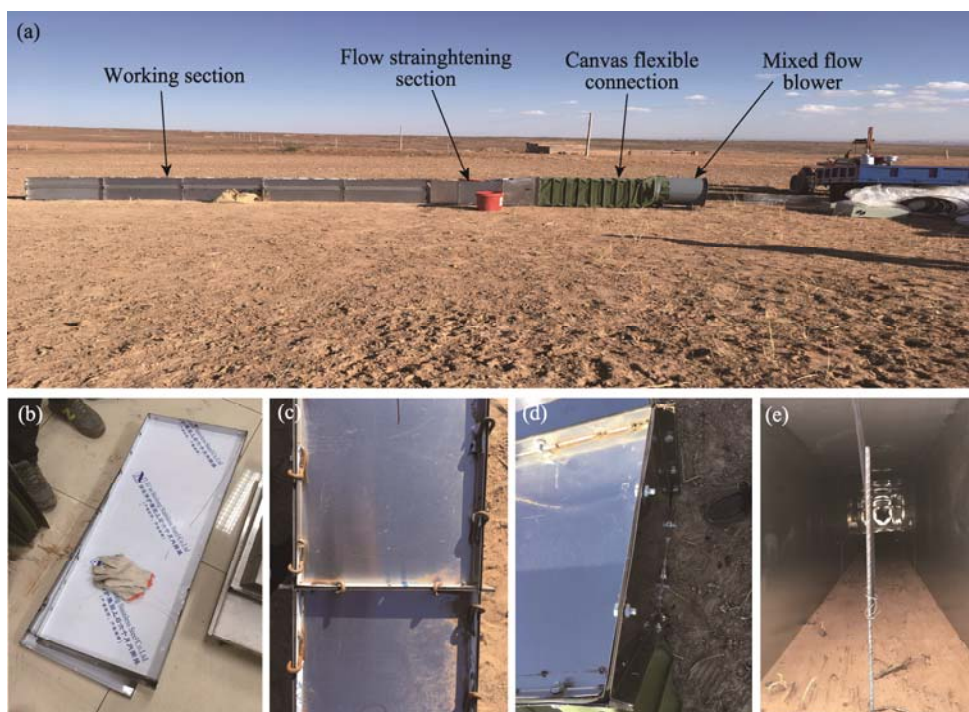


Fig. 2 Layout of the portable wind tunnel (a) with close-up views of module plate (b), assembled working section (c), assembled conditioning section (d) and inside of wind tunnel (e)

2.3 Soil sampling and analysis

Soil samples with three replicates were taken from both cropland and rangeland before the field simulated wind erosion experiments were carried out. A soil auger and sampling ring were used to collect samples to the depth of 10 cm for analyses of bulk density and primary soil particle size. Soil samples used to determine the water content were taken from the surface soil layer (0–3 cm) and subsurface soil layer (3–10 cm) because there is an appreciable difference of water content between these two layers. The undisturbed soil samples for the dry aggregate analysis were taken and parceled using a rectangular aluminum specimen box (17 cm long, 10 cm wide and 5 cm deep). The box cut into the soil like a sampling ring. Then the box was dug out from the surrounding soil using a spade, and the excess soil was removed from the box. The soil in the box was considered as the undisturbed sample. All soil samples were taken to the laboratory for physical analyses.

Soil water content and bulk density were obtained by the gravimetric method (ISSAS, 1978). Primary particle size distribution of soil was determined from dispersed soil samples using a Mastersizer 2000 laser diffraction analyzer (Malvern Instruments Ltd., Malvern, UK). The preparation of primary particle size analysis was as follows. A subsample containing about 0.5–0.8 g of soil was pre-treated with 20 mL of 30% H_2O_2 to remove organic matter. Then, it was boiled with 10 mL of 10% HCl to remove carbonates. Finally, it was washed in distilled H_2O . The

sample was then dispersed with 10 mL of 0.05 mol/L (NaPO₃)₆ before taking measurements. Dry particle size distribution of the eroded sediment collected in the field simulated wind erosion experiments was determined using an S3500 particle size analyzer (Microtrac Ltd., New York, USA) with a dry powder dispersion system. The eroded sediment samples for dry particle size distribution analysis were sieved with a 1-mm mesh sieve to remove plant residue and sheep excrement. Dry aggregate size distribution of undisturbed soil samples was measured using the dry sieving method (ISSAS, 1978). The undisturbed soil samples were air-dried firstly and water content of the air-dried soil samples was measured. Then, the air-dried soil samples were sieved through a set of six sieves (diameters of 5.00, 2.00, 1.00, 0.80, 0.50, 0.25 mm), which were shaken by a standard test sieve shaker with moderate amplitude for 0.5 and 5.0 min, respectively. After sieving, each size fraction was weighed separately. The results of the 0.5-min sieving were used to calculate the wind erodible fraction. As suggested by Campbell et al. (1993), the particle diameter of the wind erodible fraction was <0.84 mm. In this study, particle with diameter being lower than 0.80 mm was considered as wind erodible fraction. The dry aggregate stability was given by the change in erodible fraction from 0.5-min sieving to 5.0-min sieving.

2.4 Data analysis

In this study, the volume mean diameter (MDV) was calculated to quantify the dry particle size distribution of the eroded sediment:

$$\text{MDV} = \sum x_i v_i, \quad (1)$$

where x_i is the mean diameter of the i^{th} particle size range (mm), and v_i is the volume percentage of the i^{th} particle size range (%), which represented as a percentage of the total sample. In this study, the value of MDV was directly obtained from test result.

Wind erosion rate (Q) was calculated from weight of the eroded sediment using Equation 2:

$$Q = \frac{W}{A \times T}, \quad (2)$$

where W is the weight of the eroded sediment (g); A is the area of soil surface which suffered wind erosion (m²); and T is the duration of simulated blowing event (min).

The erodible fraction (EF) of the soil was calculated using Equation 3:

$$\text{EF} = \frac{W_{<0.8}}{TW} \times 100, \quad (3)$$

where EF is the erodible fraction of the soil (%); $W_{<0.8}$ is the weight of aggregates with diameter <0.8 mm (g); and TW is the initial weight of total samples (g).

The dry aggregate stability (DAS) was given by the change in erodible fraction from 0.5-min sieving to 5.0-min sieving, as shown in Equation 4:

$$\text{DAS} = \frac{W_{>0.8(0.5)} - W_{>0.8(5.0)}}{W_{>0.8(0.5)}} \times 100, \quad (4)$$

where $W_{>0.8(0.5)}$ is the weight of aggregates that retained above the 0.8-mm sieve after a 0.5-min sieving (g), and $W_{>0.8(5.0)}$ is the weight of aggregates that retained above the 0.8-mm sieve after a 5.0-min sieving (g).

To describe the temporal variation in successive wind erosion events, Shao (2008) introduced the parameter σ to indicate the exhaustion of entrainable particles. The values of σ are indices of the fractional decrease of wind erosion rate (Q) and dust (PM₁₀) emission rate (E) as a function of the successive wind erosion events, expressing as Equations 5 and 6:

$$\sigma_Q = \frac{Q_i}{Q_1} = \frac{W_i}{W_1}, \quad (5)$$

$$\sigma_E = \frac{E_i}{E_1}, \quad (6)$$

where W_i is the weight of the eroded sediment during the i^{th} wind erosion event (g); E_i is the dust (PM_{10}) emission rate of the i^{th} wind erosion event ($\text{mg}/(\text{m}^2\cdot\text{s})$); W_1 is the weight of the eroded sediment during the first wind erosion event (g); and E_1 is the dust (PM_{10}) emission rate of the first wind erosion event ($\text{mg}/(\text{m}^2\cdot\text{s})$).

In this study, the difference of soil properties between treatments were tested by the one-way ANOVA. Difference was considered significant at the $P<0.05$ level. Mean values were compared using LSD (Least-Significant Difference).

3 Results and discussion

3.1 Wind erosion rate

The field simulated wind erosion experiments showed different soil loss levels and trends as wind speed varied (Fig. 3). Specifically, at the wind speed of 8 m/s, the wind erosion rate of NTC was far lower than those of TR and TC, which were almost at the same level. When the wind speed was increased from 8 to 12 m/s, the wind erosion rates of NTC, TC and TR were multiplied by 8.7, 1.7 and 65 times, respectively, and the NTC and TC almost had the similar erosion rate. When the wind speed was increased from 12 to 16 m/s, the wind erosion rates of NTC, TC and TR were multiplied by 4.6, 1.5 and 2.5 times, respectively, and the erosion rate of TR was significantly higher than those of TC and NTC.

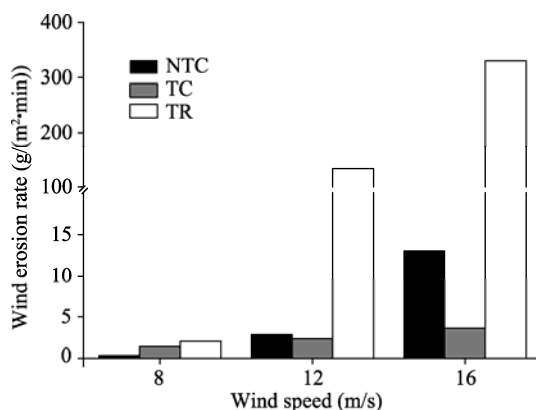


Fig. 3 Wind erosion rates of NTC (non-tilled cropland), TC (tilled cropland) and TR (trampled rangeland) at different wind speeds

The higher wind erosion rate of TR than NTC and TC was confirmed by the differences in soil physical properties (Table 1) and primary particle size composition (Table 2) between cropland and rangeland. Soils in both cropland and rangeland were classified as sandy clay loam (USDA soil texture classification). However, there were significant differences in soil particle size composition between cropland and rangeland. The particle size distribution of soil may change over time due to the winnowing process. The coarser soil texture in rangeland exhibited by high sand content may be related to the long-term influence of trampling, which resulted in the uplift of fine particles from the soil surface into the atmosphere by wind erosion (Churchman et al., 2010). Thus, the wind erosion rate of TR was higher than that of NTC.

In this study, the lowest wind erosion rate of TC at the high wind speed (Fig. 3) is inconsistent with some previous results. For example, Liu et al. (2003, 2007) found that tillage can significantly increase wind erosion. Our finding of an unexpected reduction of wind erosion after tillage may be caused by the differences of soil water content. In this study, the water contents of subsurface soil in both cropland and rangeland were much higher than those of surface soil because of a precipitation event occurred nine days before the field simulated wind erosion experiments. The evaporation and infiltration of surface soil water resulted in the water content of subsurface soil being higher than that of surface soil. Water content of surface soil before tillage

was close to the value of air-dried soil sample. However, the water content of surface soil will become higher after tillage. Soil water content is a critical factor in the reduction of wind erodibility (Webb and McGowan, 2009). The experiments of Wiggs et al. (2004) showed that aeolian sand transport is sensitive to small changes in soil moisture content and that the entrainment of particles is unlikely above a moisture threshold of 4%–6%. These findings could explain why the TC had low wind erosion rate at high wind speeds (12 and 16 m/s).

Table 1 Soil physical properties of the selected cropland and rangeland

Land-use type	Treatment	Water content of subsurface soil (%)	Water content of surface soil (%)	Water content of air-dried soil (%)	Soil bulk density (g/cm ³)	Wind erodible fraction (%)	Soil aggregate stability (%)
Cropland	NTC	7.85±0.94 ^a	0.97±0.31 ^a	0.74±0.05 ^a	1.32±0.09 ^c	62.05±8.25 ^b	78.27±6.05 ^{ab}
	TC	–	–	–	1.19±0.07 ^b	77.37±3.56 ^a	82.82±2.63 ^a
Rangeland	TR	6.29±1.31 ^b	0.82±0.31 ^a	0.65±0.05 ^a	1.51±0.02 ^a	66.01±7.63 ^b	72.50±6.46 ^b

Note: Mean±SD. Different lowercase letters within the same column indicate significant difference among treatments at the $P<0.05$ level. –, no data.

Table 2 Primary soil particle size composition in cropland and rangeland

Land-use type	Texture	Clay content (<2 µm)	Silt content (2–50 µm)	Sand content (50–1000 µm)
		(%)		
Cropland	Sandy clay loam	1.81±0.19 ^a	28.33±1.77 ^a	69.86±1.96 ^a
Rangeland	Sandy clay loam	1.48±0.20 ^a	22.52±3.38 ^b	76.00±3.55 ^b

Note: Mean±SD. Different lowercase letters within the same column indicate significant difference among land-use types at the $P<0.05$ level.

The determination of dry aggregate size distribution is another widely-used method for studying the wind erosion (Kemper and Rosenau, 1986). Campbell et al. (1993) determined that the particle diameter of the wind erodible fraction is <0.84 mm. The main properties of dry soil aggregates that indicate their susceptibility to wind erosion are stability. As shown in Table 1, the wind erodible fraction of rangeland was higher than that of cropland, while the soil aggregate stability of rangeland was lower than that of cropland. Generally speaking, the constituents of soil aggregates are the outcome of many aggregate-forming and aggregate-degrading processes (Skidmore and Layton, 1992). The higher non-erodible fraction and aggregate stability for cropland than for rangeland are related to the higher fine particle proportion (clay and silt content) in cropland, which is considered to be one of the significant cementing factors in soil aggregation (Tisdall and Oades, 1982; Amézketa, 1999). Previous studies have shown that long-term grazing could reduce soil aggregation (Hiernaux et al., 1999; Steffens et al., 2008; Zhou et al., 2010). Moreover, mechanical tillage operations and stubble grazing intensity also have immediate and direct influences on soil aggregation (Tanner et al., 2016), leading to the increase of the eroded sediment in the surface soil (Fister and Ries, 2009; Baddock et al., 2011). Tanner et al. (2016) found that wind erosion rates were higher in grazing plots than in tillage plots at high wind speeds. Similar results were found in our study, that is, the TR was more susceptible to higher wind erosivity (wind speeds of 12 and 16 m/s) than the TC. There are two possible reasons. First, trampling is a day-by-day activity, which may generate more impacts on soil than tilling (an occasional activity). Second, tillage may increase the water content of surface soil, thereby reducing wind erosion.

3.2 Particle size characteristics of the eroded sediment

The values of volume mean diameter of the collected eroded sediment are shown in Figure 4. As expected, the volume mean diameter of the eroded sediment generally increased with increasing of wind speed in all soil surface conditions. However, the trends of the values differed between treatments. Generally speaking, the variations of volume mean diameter of the eroded sediment along with the increasing of wind speed were similar with those of wind erosion rate. For TR, the greatest volume mean diameter of the eroded sediment was observed at the highest wind erosion rate (corresponding to wind speed of 16 m/s); and for NTC, the lowest volume mean diameter of

the eroded sediment was observed at the lowest wind erosion rate (corresponding to wind speed of 8 m/s). The variations in the volume mean diameter could reflect how air flow entrains different size particles at different wind speeds. Apart from the different modes of transport (sand in saltation and dust in suspension), selective aeolian entrainment with respect to grain size is an important aspect of particle transportation (Flores-Aqueveque et al., 2010).

Figure 5 shows the clay and silt content of the eroded sediment. The clay and silt content showed an opposite trend with the volume mean diameter of the eroded sediment and wind erosion rate. As shown in Figure 5, the higher the wind speed, the lower the clay and silt content in the eroded sediment. In other words, as wind speed increases, the proportion of coarse particles was generally higher than the proportion of fine particles in the eroded sediment. This selective effect of wind erosion occurs during the processes of entrainment, transportation, and deposition. At the lower wind speeds, the selective effect occurs during entrainment as only smaller fine particles become windborne. At the higher wind speeds, all the soil particles can be entrained. The same processes should be manifest in the transport and deposition phases of wind erosion.

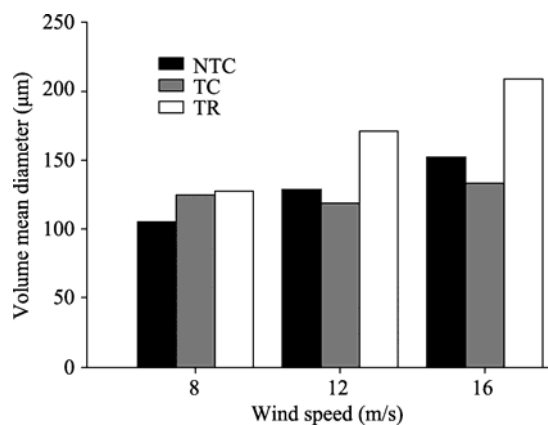


Fig. 4 Volume mean diameter of the eroded sediment in NTC, TC, and TR at different wind speeds

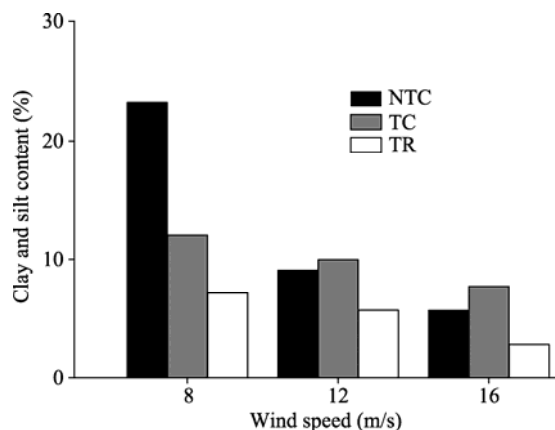


Fig. 5 Clay and silt content of the eroded sediment in NTC, TC, and TR at different wind speeds

3.3 Temporal variation of wind erosion

To investigate the temporal variation of wind erosion, indicated by the amount of the eroded sediment, we analyzed the mean and maximum emission rates of PM₁₀ for TR, which had a much higher wind erosion rate. The results are shown in Figure 6. The soil loss peaked during the first blowing session and subsequently decreased rapidly at each wind speed. Liu et al. (2003) suggested that soil loss decreases exponentially with respect to the successive blowing and the decrease depends mainly on the erodible particles and structural condition of the soil. In this study,

we found the effect of wind speed on erosion from the soil surface in TR: the greater the wind speed, the faster the wind erosion rate decreased with erosion time. This indicates that the less blowing time is required for erodible particles to be deflated at the high wind speeds. Soil loss decreased unevenly during wind erosion events. The maximum and mean emission rates of PM_{10} in the five successive wind erosion events are shown in Figures 6b and c, respectively. The mean emission rate of PM_{10} ranged from 0.07 (the fifth 2-min blowing event with wind speed of 8 m/s) to 91.20 $\text{mg}/(\text{m}^2\cdot\text{s})$ (the first 2-min blowing event with wind speed of 16 m/s). Our findings are consistent with the results of Zhang et al. (2016), who studied the mechanisms of dust emission and concluded that dust was entrained in the first 2–3 min of the simulated wind erosion experiments if the dust supply was unlimited. The surface renewal process is an important mechanism that affects dust emission.

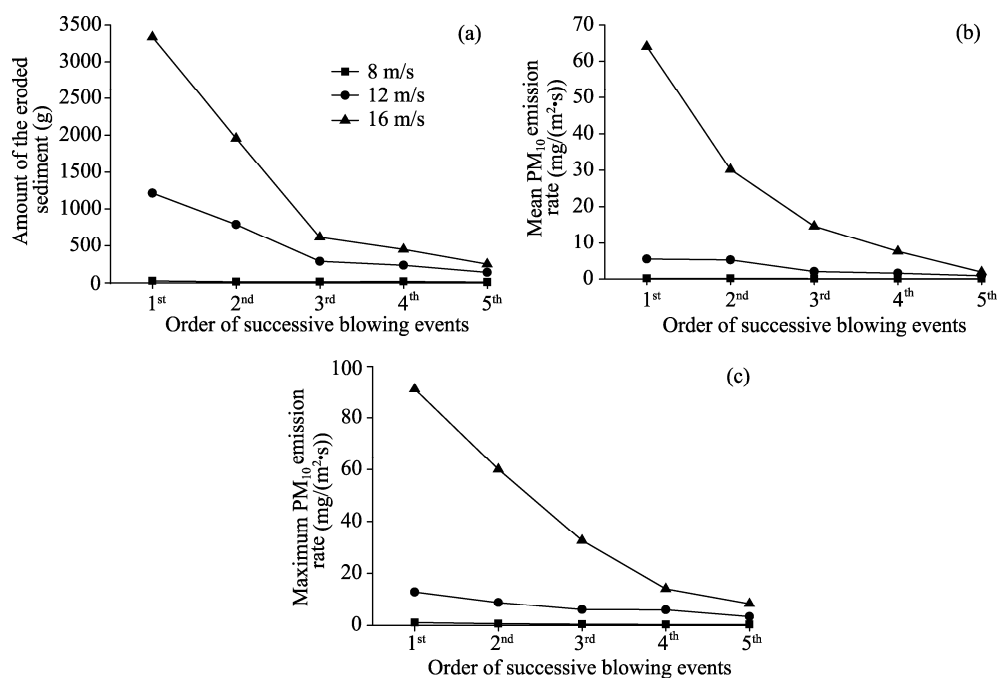


Fig. 6 Temporal variations of the amount of the eroded sediment (a), the mean PM_{10} emission rate (b) and the maximum PM_{10} emission rate of (c) in the five successive 2-min blowing events in TR. Note that values of horizontal axis represent the order of the five successive 2-min blowing events.

The σ values in our study are presented in Table 3. The results show that at the wind speeds of 8 and 16 m/s, the σ values of the wind erosion rate and PM_{10} emission rate decreased quickly until the end of the second 2-min blowing event. At the wind speed of 12 m/s, there was also a rapid decrease in the σ values during the third 2-min blowing event. These results indicate that the erodible soil particles are mainly exhausted in the first and second 2-min blowing events. The complete exhaustion of erodible particles will occur sooner or later, depending on both the wind erosion rate and the supply of fine particles. Grini et al. (2002) explained that the emission of fine particulate matter was sustained from the fine textured soils in the successive wind erosion events due to the high content of PM_{10} in soil aggregates. The fine particles are available for entrainment over longer time periods. However, in the coarse textured soils, the PM_{10} particles with low content in non-aggregated soil are loose or lightly bonded to sand grains, and thus they are rapidly depleted by the saltation process (Panebianco et al., 2016).

4 Conclusions

We investigated wind erosion under different soil disturbances in Yanchi County, using a portable wind tunnel. Compared with rangeland soil, the cropland soil had lower bulk density, higher water

Table 3 σ values of the wind erosion rate and PM₁₀ emission rate in the five successive 2-min blowing events in TR at different wind speeds

Order of successive blowing events	σ								
	Wind erosion rate			Maximum PM ₁₀ emission rate			Mean PM ₁₀ emission rate		
	8 m/s	12 m/s	16 m/s	8 m/s	12 m/s	16 m/s	8 m/s	12 m/s	16 m/s
1 st	1.00	1.00	1.00	1.00	1.00	1.00	1.00	1.00	1.00
2 nd	0.53	0.65	0.59	0.62	0.95	0.47	0.53	0.69	0.66
3 rd	0.45	0.24	0.18	0.52	0.36	0.23	0.25	0.47	0.36
4 th	0.35	0.19	0.13	0.46	0.28	0.12	0.18	0.46	0.15
5 th	0.21	0.11	0.07	0.45	0.15	0.03	0.15	0.25	0.09

holding capacity, and higher clay and silt content. As the wind speed increased from 8 to 16 m/s, the wind erosion rate increased sharply for TR, remained almost steady for TC, and increased moderately for NTC. An unexpected reduction in wind erosion was found in TC at the wind speeds of 12 and 16 m/s, with the wind erosion rate being lowest in TC among the three treatments. With increasing of wind speed, the volume mean diameter of the eroded sediment generally increased while the clay and silt content decreased in all soil surface conditions. For a series of successive wind erosion events in TR, the wind erosion rate and PM₁₀ emission rate decreased with erosion time due to the exhaustion of erodible particles.

Acknowledgements

This research was supported by the National Natural Science Foundation of China (41401310, 41661003) and the Science-Technology Research Project of Ningxia Environmental Protection Department. We thank the editors and three anonymous reviewers for their constructive comments and suggestions for the improvement of this paper.

References

- Amézqueta E. 1999. Soil aggregate stability: a review. *Journal of Sustainable Agriculture*, 14(2–3): 83–151.
- Baddock M C, Zobeck T M, Van Pel R S, et al. 2011. Dust emissions from undisturbed and disturbed, crusted playa surfaces: cattle trampling effects. *Aeolian Research*, 3(1): 31–41.
- Belnap J, Phillips S L, Herrick J E, et al. 2007. Wind erodibility of soils at Fort Irwin, California (Mojave Desert), USA, before and after trampling disturbance: implications for land management. *Earth Surface Processes and Landforms*, 32(1): 75–84.
- Campbell C A, Curtin D, Zentner R P, et al. 1993. Soil aggregation as influenced by cultural practices in Saskatchewan: II. Brown and dark brown chernozemic soils. *Canadian Journal of Soil Science*, 73(4): 597–612.
- Chepil W S. 1953. Field structure of cultivated soils with special reference to erodibility by wind. *Soil Science Society of America Journal*, 17(3): 185–190.
- Chepil W S, Woodruff N P. 1954. Estimations of wind erodibility of field surfaces. *Journal of Soil and Water Conservation*, 9(6): 257–265.
- Churchman G J, Foster R C, D'Acqui L P, et al. 2010. Effect of land-use history on the potential for carbon sequestration in an Alfisol. *Soil and Tillage Research*, 109(1): 23–35.
- Colazo J C, Buschiazio D E. 2010. Soil dry aggregate stability and wind erodible fraction in a semiarid environment of Argentina. *Geoderma*, 159(1–2): 228–236.
- Dong Z B, Wang X M, Liu L Y. 2000. Wind erosion in arid and semiarid China: an overview. *Journal of Soil and Water Conservation*, 55(4): 439–444.
- Fister W, Ries J B. 2009. Wind erosion in the central Ebro Basin under changing land use management. Field experiments with a portable wind tunnel. *Journal of Arid Environments*, 73(11): 996–1004.
- Flores-Aqueveque V, Alfaro S, Muñoz R, et al. 2010. Aeolian erosion and sand transport over the Mejillones Pampa in the coastal Atacama Desert of northern Chile. *Geomorphology*, 120(3–4): 312–325.
- Fryrear D W. 1981. Management of blank rows in dryland skip-row cotton. *Transactions of the ASAE*, 24(4): 988–990.
- Gao Y, Dang X H, Yu Y, et al. 2016. Effects of tillage methods on soil carbon and wind erosion. *Land Degradation & Development*, 27(3): 583–591.
- Grini A, Zender C S, Colarco P R. 2002. Saltation sandblasting behavior during mineral dust aerosol production. *Geophysical*

- Research Letters, 29(18): 1868.
- Hiernaux P, Biélders C L, Valentin C, et al. 1999. Effects of livestock grazing on physical and chemical properties of sandy soils in Sahelian rangelands. *Journal of Arid Environments*, 41(3): 231–245.
- Institute of Soil Science, Chinese Academy of Science (ISSAS). 1978. *Soil Physical and Chemical Analysis*. Shanghai: Shanghai Science and Technology Press, 514–518. (in Chinese)
- Kemper W D, Rosenau R C. 1986. Aggregate stability and size distribution. In: Klute A. *Methods of Soil Analysis: Part 1*. (2nd ed.). Madison (WI): ASA and SSSA: 425–442.
- Leys J F, Raupach M R. 1991. Soil flux measurements using a portable wind erosion tunnel. *Australian Journal of Soil Research*, 29(4): 533–552.
- Li J R, Okin G S, Epstein H E. 2015. Effects of enhanced wind erosion on surface soil texture and characteristics of windblown sediments. *Journal of Geophysical Research: Biogeosciences*, 114(G2): G02003.
- Li X Y, Liu L Y, Wang J H. 2004. Wind tunnel simulation of aeolian sandy soil erodibility under human disturbance. *Geomorphology*, 59(1–4): 3–11.
- Liu B, Zhao W Z, Liu Z L, et al. 2015. Changes in species diversity, aboveground biomass, and vegetation cover along an afforestation successional gradient in a semiarid desert steppe of China. *Ecological Engineering*, 81: 301–311.
- Liu L Y, Shi P J, Zou X Y, et al. 2003. Short-term dynamics of wind erosion of three newly cultivated grassland soils in Northern China. *Geoderma*, 115(1–2): 55–64.
- Liu L Y, Li X Y, Shi P J, et al. 2007. Wind erodibility of major soils in the farming–pastoral ecotone of China. *Journal of Arid Environments*, 68(4): 611–623.
- Panebianco J, Mendez M, Buschiazio D E. 2016. PM₁₀ emission, sandblasting efficiency and vertical entrainment during successive wind-erosion events: a wind-tunnel approach. *Boundary-Layer Meteorology*, 161(2): 335–353.
- Segovia C, Gómez J D, Gallardo P, et al. 2017. Soil nutrients losses by wind erosion in a citrus crop at southeast Spain. *Eurasian Soil Science*, 50(6): 756–763.
- Shao Y P. 2008. *Physics and Modelling of Wind Erosion*. Heidelberg: Springer, 199–212.
- Sharratt B, Wendling L, Feng G L. 2010. Windblown dust affected by tillage intensity during summer fallow. *Aeolian Research*, 2(2–3): 129–134.
- Sharratt B, Strom L, Pressley S. 2015. Nitrogen loss from windblown agricultural soils in the Columbia Plateau. *Aeolian Research*, 18: 47–53.
- Singh P, Sharratt B, Schillinger W F. 2012. Wind erosion and PM₁₀ emission affected by tillage systems in the world's driest rainfed wheat region. *Soil and Tillage Research*, 124: 219–225.
- Skidmore E L, Layton J B. 1992. Dry-soil aggregate stability as influenced by selected soil properties. *Soil Science Society of America Journal*, 56(2): 557–561.
- State Forestry Administration, PR China. 2015. A bulletin of status quo of desertification and sandification in China. [2015-12-29]. <http://www.forestry.gov.cn/main/69/content-831684.html>.
- Steffens M, Kölbl A, Totsche K U, et al. 2008. Grazing effects on soil chemical and physical properties in a semiarid steppe of Inner Mongolia (P.R. China). *Geoderma*, 143(1–2): 63–72.
- Tang Z S, Hui A, Lei D, et al. 2016. Effect of desertification on productivity in a desert steppe. *Nature Scientific Reports*, 6: 27839.
- Tanner S, Katra I, Haim A, et al. 2016. Short-term soil loss by eolian erosion in response to different rain-fed agricultural practices. *Soil and Tillage Research*, 155: 149–156.
- Tisdall J M, Oades J M. 1982. Organic matter and water-stable aggregates in soils. *European Journal of Soil Science*, 33(2): 141–163.
- Van Pelt R S, Baddock M C, Zobeck T M, et al. 2013. Field wind tunnel testing of two silt loam soils on the North American Central High Plains. *Aeolian Research*, 10: 53–59.
- Wang T, Song X, Yan C Z, et al. 2011. Remote sensing analysis on aeolian desertification trends in northern China during 1975–2010. *Journal of Desert Research*, 31(6): 1351–1356. (in Chinese)
- Wang X M, Chen F H, Hasi E, et al. 2008. Desertification in China: an assessment. *Earth-Science Reviews*, 88(3–4): 188–206.
- Webb N P, McGowan H A. 2009. Approaches to modelling land erodibility by wind. *Progress in Physical Geography*, 33(5): 587–613.
- Wiggs G F S, Baird A J, Atherton R J. 2004. The dynamic effects of moisture on the entrainment and transport of sand by wind. *Geomorphology*, 59(1–4): 13–30.
- Yan Y C, Tang H P, Zhang X S, et al. 2010. A probe into grassland wind erosion based on the analysis of soil particle size. *Journal of Desert Research*, 30(6): 1263–1268. (in Chinese)

- Yang F B, Lu C H. 2016. Assessing changes in wind erosion climatic erosivity in China's dryland region during 1961–2012. *Journal of Geographical Sciences*, 26(9): 1263–1276.
- Zhang J, Teng Z J, Huang N, et al. 2016. Surface renewal as a significant mechanism for dust emission. *Atmospheric Chemistry and Physics*, 16(24): 15517–15528.
- Zhang Z C, Dong Z B, Chen S Y. 2013. Wind erodibility in eastern Ningxia Province, China. *Environmental Earth Sciences*, 68(8): 2263–2270.
- Zhao W Z, Xiao H L, Liu Z M, et al. 2005. Soil degradation and restoration as affected by land use change in the semiarid Bashang area, northern China. *CATENA*, 59(2): 173–186.
- Zhou T R, Zhang L S. 1992. Holocene Environment Evolution and Prediction of the Farming-Pastoral Ecotone in China. Beijing: Geological Press, 121–146. (in Chinese)
- Zhou Z C, Gan Z T, Shanguan Z P, et al. 2010. Effects of grazing on soil physical properties and soil erodibility in semiarid grassland of the Northern Loess Plateau (China). *CATENA*, 82(2): 87–91.
- Zhu Z D, Chen G T. 1994. Sandy Desertification in China. Beijing: Science Press, 157–159. (in Chinese)
- Zobeck T M, Popham T W. 1990. Dry aggregate size distribution of sandy soils as influenced by tillage and precipitation. *Soil Science Society of America Journal*, 54(1) 198–204.
- Zobeck T M, Van Pelt R S. 2011. Wind erosion. In: Hatfield J L, Sauer T J. *Soil Management: Building a Stable Base for Agriculture*. Madison, USA: American Society of Agronomy and Soil Science Society of America, 209–227.